



Chloride-salinity as indicator of the chemical composition of groundwater: empirical predictive model based on aquifers in Southern Quebec, Canada

Lamine Boumaiza^{1,2} · Julien Walter^{1,2} · Romain Chesnaux^{1,2} · Randy L. Stotler³ · Tao Wen⁴ · Karen H. Johannesson⁵ · Karthikeyan Brindha⁶ · Frédéric Huneau^{7,8}

Received: 18 January 2022 / Accepted: 18 March 2022

© The Author(s), under exclusive licence to Springer-Verlag GmbH Germany, part of Springer Nature 2022

Abstract

The present study first describes the variations in concentrations of 12 chemical elements in groundwater relative to salinity levels in Southern Quebec (Canada) groundwater systems, and then uses this data to develop an empirical predictive model for evaluating groundwater chemical composition relative to salinity levels. Data is drawn from a large groundwater chemistry database containing 2608 samples. Eight salinity classes were established from lowest to highest chloride (Cl) concentrations. Graphical analyses were applied to describe variations in major, minor, and trace element concentrations relative to salinity levels. Results show that the major elements were found to be dominant in the lower salinity classes, whereas Cl becomes dominant at the highest salinity classes. For each of the major elements, a transitional state was identified between domination of the major elements and domination of Cl. This transition occurred at a different level of salinity for each of the major elements. Except for Si, the minor elements Ba, B, and Sr generally increase relative to the increase of Cl. The highest Mn concentrations were found to be associated with only the highest levels of Cl, whereas F was observed to be more abundant than Mn. Based on this analysis of the data, a correlation table was established between salinity level and concentrations of the chemical constituents. We thus propose a predictive empirical model, identifying a profile of the chemical composition of groundwater relative to salinity levels, to help homeowners and groundwater managers evaluate groundwater quality before resorting to laborious and costly laboratory analyses.

Keywords Hydrogeochemistry · Groundwater · Salinity · Major and minor elements · Trace elements · Canada

Introduction

The uncontrolled exploitation of groundwater in combination with other anthropogenic activities has led to a severe deterioration of groundwater quality throughout the world (Seddiq et al. 2019; Zendehbad et al. 2019; Boumaiza

et al. 2020a). Geogenic processes also exert a significant impact on groundwater quality (Swartz et al. 2004; Bondu et al. 2018). Programs have been implemented throughout the world, at local, regional, and national scales, to assess and monitor groundwater quality and to evaluate the potential for anthropogenic and/or natural groundwater contamination (Leahy and Thompson 1994; Koreimann et al.

Responsible Editor: Marcus Schulz

✉ Lamine Boumaiza
lamine.boumaiza@uqac.ca

¹ Département Des Sciences Appliquées, Université du Québec À Chicoutimi, Saguenay, QC G7H 2B1, Canada

² Centre d'études Sur Les Ressources Minérales, Groupe de Recherche Risque Ressource Eau, Université du Québec À Chicoutimi, Saguenay, QC G7H 2B1, Canada

³ Department of Earth and Environmental Sciences, University of Waterloo, Waterloo, ON N2T 0A4, Canada

⁴ Department of Earth and Environmental Sciences, Syracuse University, Syracuse, NY 13244, USA

⁵ School for the Environment, University of Massachusetts Boston, Boston, MA 02125, USA

⁶ Hydrogeology Group, Institute of Geological Sciences, Freie Universität Berlin, 12249 Berlin, Germany

⁷ Département d'Hydrogéologie, Université de Corse Pascal Paoli, Campus Grimaldi, 20250 Corte, France

⁸ UMR 6134, SPE, CNRS, BP 52, 20250 Corte, France

1996; Foster et al. 2006; Evans et al. 2012; Barbieri et al. 2019; Ricolfi et al. 2020). In Canada, several regional studies have recently been conducted with the aim of assessing the quality of groundwater in different provinces (e.g., Cui and Wei 2000; NBDE 2008; Kennedy and Drage 2009; Hamilton et al. 2015). In the Province of Quebec in Canada, where more than 2 million people rely on groundwater for their drinking water supply (Larocque et al. 2018), the assessment of regional groundwater quality is supported by the Groundwater Knowledge Acquisition Program (*Programme d'acquisition de connaissances sur les eaux souterraines*, PACES). This program was implemented in 2009 by the Quebec Ministry of the Environment (*Ministère de l'Environnement et de la Lutte contre les Changements Climatiques*, MELCC) to provide an integrated portrait of groundwater resources in Southern Quebec in terms of both quantity and quality, and to better protect and sustainably manage groundwater resources in Quebec (Rouleau et al. 2012; Larocque et al. 2018; MELCC 2021). The multi-faceted PACES program has developed alternative methods for assessing the vulnerability of aquifers, simulating groundwater flow, numerically estimating groundwater travel times, quantifying groundwater recharge, characterizing the internal architecture of aquifers, evaluating specific aquifer properties, and understanding the chemical evolution of groundwater within aquifers (Chesnaux et al. 2011; Boumaiza et al. 2015 2017; Montcoudiol et al. 2015; Boumaiza et al. 2019 2020c b 2021a 2021c 2021b 2022; Walter et al. 2017; Ferroud et al. 2018 2019; Nadeau et al. 2018; Chesnaux and Stumpp 2018; Labrecque et al. 2020).

The PACES program has provided insight into the wide variability of groundwater quality in Southern Quebec, in both shallow unconfined aquifers and deeper confined aquifers. For example, concentrations of chloride (Cl) in groundwater have ranged from values well below the detection limit (<0.1 mg/L) to a very high value of 15,000 mg/L (MELCC 2021). Saline water that is typically found in deeper aquifers (> 1000 m) is also found at shallow depths (< 100 m)—both in fractured rock and in unconsolidated aquifers—as the result of a long vertical upward flow through discontinuities and faults (Rouleau et al. 2013; Wen et al. 2015). High Cl intake can cause high levels of Cl in the bloodstream, a condition called hyperchloremia. Furthermore, at relatively low concentrations, Cl can affect the taste of drinking water. In fact, when freshwater is mixed with saltwater in as low a proportion as 1% (corresponding to ≈ 250 mg/L of Cl), it becomes unfit for drinking (WHO 2017). Around the world, high salinity levels in groundwater have commonly been associated with high levels of numerous inorganic chemical constituents (Deng et al. 2009; Rango et al. 2013; Vikas et al. 2013; Avrahamov et al. 2014; Santucci et al. 2016; Elumalai et al. 2019) such as fluoride and boron; both of these can pose a health risk to humans at high concentrations.

Fluoride is a known xenobiotic; its impact on human health occurs through fluorosis (Zango et al. 2019). Fluoride is suspected to be associated with other adverse health effects, including ligament calcification, liver and kidney dysfunction, developmental disorder in children, and neurological weakness (Ding et al. 2011; Yadav et al. 2019; Yang et al. 2020). Exposure to large amounts of boron (approximately 30 g of boric acid) over short periods of time can affect the stomach, intestines, liver, kidney, and brain and can eventually lead to death (ATSDR 2010).

In Quebec, a number of PACES-supported hydrogeochemical studies have reported the presence of high concentrations of various chemical constituents in groundwater (Beaudry 2013; Blanchette et al. 2010; Bondu et al. 2018 2020; Chaillou et al. 2018; Meyzonnat et al. 2016; Minet et al. 2017; Montcoudiol et al. 2015; Walter et al. 2019). To fill in some of the remaining knowledge gaps, further studies are needed to draw a comprehensive portrait of the variations in concentrations of the different mineral constituents in groundwater, in particular relative to salinity levels. Knowledge of salinity levels is helpful for characterizing the flow, chemical evolution, and mixing/migration patterns of groundwater within aquifer systems; it may also shed light on the vulnerability of groundwater to anthropogenic contamination (Grassi and Netti 2000; Williams et al. 2000; Lazur et al. 2020; Mora et al. 2020). Accordingly, the first objective of the present study is to describe the variability of chemical composition of groundwater in Southern Quebec in regards to its salinity levels. In this study, “chemical composition” of groundwater designates the concentration of inorganic elements in groundwater, whereas the term “salinity” refers to the Cl concentration (the terms “salinity” and “Cl concentration” are used interchangeably). Work on the first objective was based on the PACES groundwater chemistry database (MELCC 2021) which is comprised of data drawn from 2608 groundwater samples collected in sixteen regions of Southern Quebec. The PACES database includes chemical analyses of 40 inorganic constituents. However, the present study focuses on Cl concentrations with 12 other inorganic constituents (HCO_3^- , SO_4^{2-} , Ca^{2+} , Mg^{2+} , Na^+ , K^+ , B, Sr, Mn, Ba, Si, F) for which most measurements ($> 50\%$) were reported above the detection limits of each inorganic element.

In Quebec, it is the legal responsibility of homeowners whose residence is not connected to a municipal water supply (i.e., those who have their own well) to ensure the quality of their groundwater; however, homeowners are not always able to assess groundwater quality and undertake long-term monitoring owing to limited knowledge or financial means (Bondu et al. 2020). The second objective of the present study is therefore to develop an empirical groundwater predictive model, to help gain preliminary insight into the quality of groundwater; such information could be used to

support a decision to avoid or pursue expensive chemical analyses. The first objective, describing the variations in chemical concentrations and salinity levels in groundwater in Southern Quebec, is used to achieve the second objective, which consists of developing an empirical predictive groundwater quality model that establishes a relationship between the chemical composition of groundwater and its salinity level. More specifically, by linking Cl to electrical conductivity (EC), the model determines the Cl concentration of groundwater based on the value of its EC, which can easily be measured in-situ. The relationship between Cl and EC is established according to an empirical equation that was developed for this study using the PACES groundwater chemistry data. Determining the salinity level then makes it possible to predict the relative concentrations of the 12 studied chemical constituents influencing the quality of groundwater. Assuming that PACES groundwater samples were collected under equilibrium conditions, the resulting predictive model thus provides an empirical quantification, in effect a “profile,” of the chemical composition of groundwater. Studies of groundwater systems may include hydro-chemistry numerical models, which require thermodynamic

parameterization including aquifer mineralogy. Such studies are extremely complex to conduct over large territories such as Southern Quebec (100,000 km²). An empirical predictive model such as the one proposed in the present study may help draw a profile of groundwater quality and provide a useful step in integrating and summarizing groundwater data collected over large geographic areas. The predictive model is also a helpful tool to qualitatively monitor groundwater quality, to provide a portrait of the chemical evolution of groundwater, and to manage groundwater in regard to its salinity level.

Study area

Location, climate, and bedrock basement

The study area encompasses sixteen administrative regions of Southern Quebec, Canada, covering 100,000 km² (indexed as 1 to 16 in Fig. 1a). Southern Quebec, which has a humid northern climate, experiences rainy events over the summer-fall seasons (from May to October), and heavy

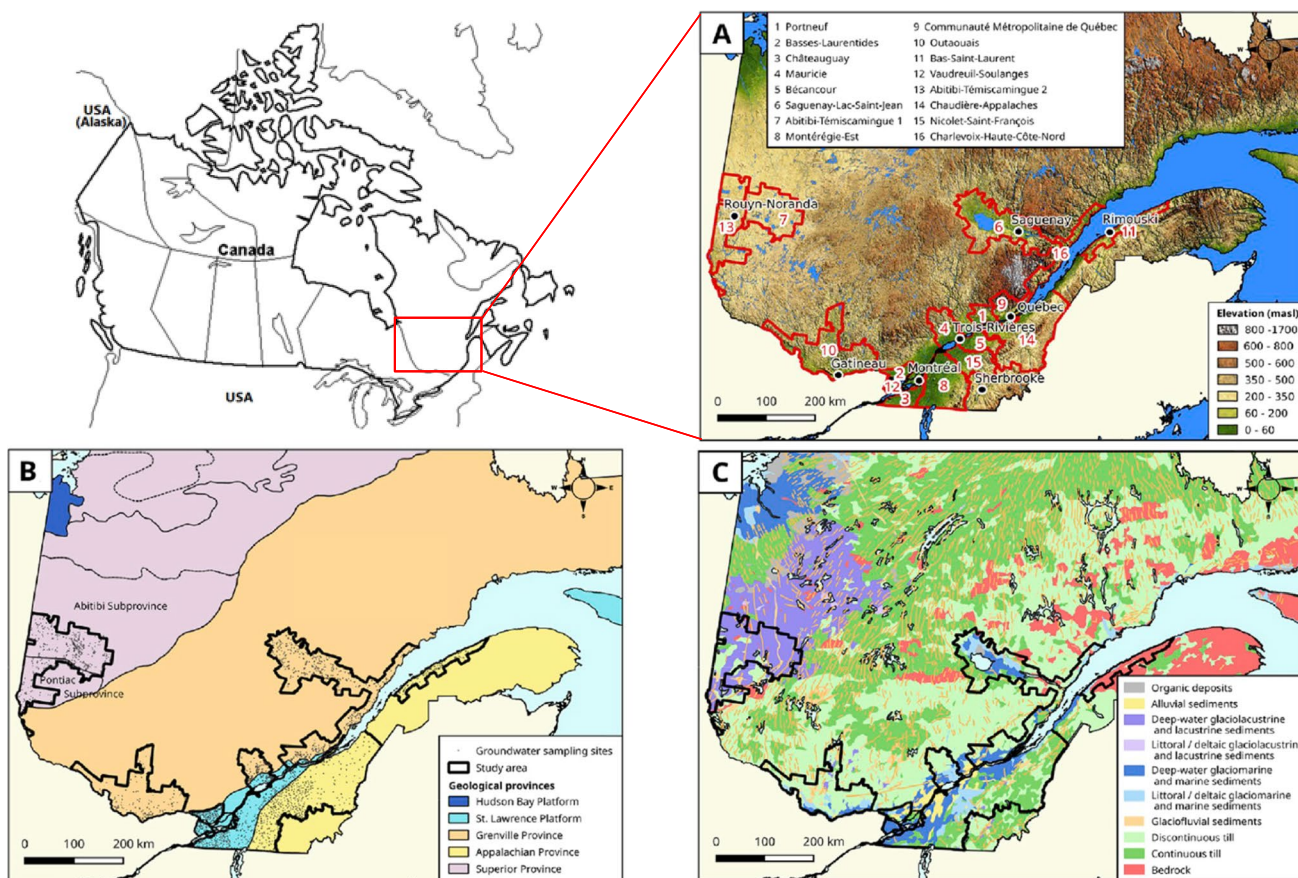


Fig. 1 a Location of the investigated study area in Quebec, Canada. The numbers 1–16 indicate the sub-regions of the study area. b Geological provinces and c surficial deposits (Bondu et al. 2020)

snow accumulation during the winter-early spring seasons (from November to March), with complete snowmelt occurring in April/May. The mean annual rainfall captured over Southern Quebec is approximately 900 mm, with a mean annual snow accumulation equivalent to 290 mm of water. The average monthly temperatures range from $-16\text{ }^{\circ}\text{C}$ in January to $+18\text{ }^{\circ}\text{C}$ in July (Government of Canada 2021). The bedrock geology of the study area belongs to four geological provinces (Fig. 1b): (i) the Archean Abitibi greenstone belonging to the Southern part of the Archean Superior Province (~ 4.3 to 2.5 billion years); (ii) the Grenville Province (~ 2.7 billion to 600 million years), which occupies a large portion of Southern Quebec; (iii) the St. Lawrence Platform (~ 570 to 430 million years) extending in a north-eastern orientation on both sides of the St. Lawrence River; and (iv) the Appalachian Province (~ 480 million years) in the southeastern part of the study area. Following the Wisconsin glacial retreat, when the glaciers deposited large accumulations of Quaternary deposits (Fig. 1c), southern Quebec was invaded by post-glacial seas and proglacial lakes. These deposits are mainly composed of boulders, gravel, sand, and clay-silt, with thicknesses ranging from several meters to tens of meters (Bolduc and Ross 2001; CERM-PACES 2013). The supply of drinking water in urbanized areas is usually drawn from unconsolidated aquifers composed of granular sediments, rather than bedrock aquifers (Dessureault 1975; Chaillou et al. 2018; Rey et al. 2018). However, in rural areas, where single-family dwellings largely rely on private domestic wells, bedrock aquifers are the major source of drinking water (Montcoudiol et al. 2015; Meyzonnat et al. 2016; Walter et al. 2018).

Hydrogeological and hydrogeochemical background

The coarse-grained sediment aquifers of the study area are commonly covered by glaciomarine and glaciolacustrine silt-clay deposits, forming confined aquifer systems (Dessureault 1975; Lamothe and St-Jacques 2014; Thibaudeau and Veillette 2005). Granular sediments are also encountered in unconfined situations, as is the case with the major valleys of the Saguenay-Lac-Saint-Jean Highlands, which were not covered by fine sediments by the invading Laflamme Sea (Walter et al. 2018 2017). Under the unconsolidated aquifers, the basement rocks are characterized by heterogeneous low permeabilities ranging from 10^{-9} to 10^{-4} m/s, wherein the groundwater flow is dominant in the fracture networks and bedding planes of the upper part (50–60 m) of the bedrock aquifers (McCormack and Therrien 2013; Rouleau et al. 2013; Benoit et al. 2014; Richard et al. 2016; Ladevèze et al. 2019). The bedrock aquifer systems are partly covered by silt and clay sediments, as in the case of glaciomarine clays in the St. Lawrence Lowlands, creating confining conditions

for the bedrock aquifer systems (Lamothe 1989; Meyzonnat et al. 2016). In the Appalachian Highlands, however, surficial granular sediments are thin; therefore, unconfined conditions prevail for most of the fractured bedrock aquifer systems (Lefebvre et al. 2015). Recharge of the bedrock aquifer systems and the of the deeper unconsolidated aquifer systems occurs mostly in the unconfined areas typically found in highlands (Meinken and Stober 1997; Cloutier et al. 2006; Chesnaux 2013; Montcoudiol et al. 2015; Walter et al. 2017; Beaudry et al. 2018; Walter 2018).

In the highland recharge areas, groundwater is characterized by low mineralization, a slightly acidic to near neutral pH and oxidizing redox potential, in which the dominant water type is Ca-HCO_3 . This is consistent with water that has recently infiltrated into the subsurface, whose features are governed by weathering of silicate (Ca-feldspar, particularly) (Beaudry et al. 2018; Chaillou et al. 2018; Ghesquière et al. 2015). This groundwater type evolves to Na-HCO_3 during subsurface migration and interacts with the post-glacial marine clay (Montcoudiol et al. 2015; Walter et al. 2019); it can be found in the semi-confined to confined aquifers under reducing conditions, as identified, for example, in the confined aquifers of south-western Quebec (Meyzonnat et al. 2016), and in the confined bedrock aquifers of the Saguenay-Lac-Saint-Jean region (Walter et al. 2017). The chemistry of groundwater tends to evolve further toward modern seawater-like compositions, i.e., Na-Cl-rich (Walter et al. 2017). This Na-Cl water type—characterized by high total dissolved solids, alkaline pH and mildly reducing to reducing redox potential—mainly occurs in confined unconsolidated/bedrock aquifers, and is widely prevalent in the study area (Cloutier et al. 2008 2010; Ghesquière et al. 2015; Lefebvre et al. 2015; Montcoudiol et al. 2015).

Materials and methods

Data overview

The PACES database contains data drawn from a total of 2608 groundwater samples collected from private, municipal, and observation wells during the summer periods as part of the 2009–2015 PACES Program; 893 samples were collected from unconsolidated aquifers and 1678 groundwater samples were obtained from bedrock aquifers (37 of the 208 samples originated from an unknown aquifer type). All groundwater samples collected in the PACES Program were analyzed by an accredited commercial laboratory (*Bureau Veritas Laboratories*) in compliance with the standard procedures of Quebec's Ministry of the Environment (CEAEQ 2021). Laboratory analyses targeted major elements (Cl, HCO_3 , SO_4 , Ca, Mg, Na, K) and some minor and trace elements (B, Sr, Mn, Ba, Si, F). Alkalinity (as CaCO_3) and

HCO₃ were determined by volumetric titration to pH 4.5 using a Mantech (Guelph, ON) PC-Titrate auto-analyzer. The anions SO₄ and Cl were measured using a Dionex (Sunnyvale, CA) ICS-1600 ion chromatograph. Major cations (Ca, Mg, Na, K), and minor/trace elements (Si, B, Ba, Mn, Sr) were analyzed by inductively coupled plasma mass spectrometry (ICP-MS) using an Agilent (Santa Clara, CA) 7700X ICP-MS. Fluoride (F) was measured using a fluoride ion-selective electrode (a complete description of each analytical method employed is available in CEAEQ (2021)). In the present study, values below the detection limit for each of the 13 selected chemical constituents were not included in the statistical analyses, to avoid including unreliable values in the statistical analysis. Quality-Assurance/Quality-Control programs were implemented that considered both field and laboratory procedures—in compliance with the standard procedures of Quebec's Ministry of the Environment (CEAEQ 2021)—with the calculation of ionic balance, for which a value of $\pm 10\%$ is considered acceptable (Hounslow 1995). The procedures included field and transport blanks, which were performed to evaluate a potential contamination from the field and/or during transportation of groundwater samples. Furthermore, field procedures included the collection of duplicate groundwater samples (DGSs) corresponding to 10% of the total collected groundwater samples. The DGSs were collected at the same time as the initial groundwater samples (IGSs), from same sampling origin, and sent to the laboratory under different identifications than those of the IGSs. Further, the collected DGSs were analyzed for selected inorganic elements, while their results were compared to those of the IGSs. Similar procedures were performed by the laboratory, which performed twice analyses for 10% of the total received IGSs, in order to evaluate the replicability of the analysis procedure. The standard deviation (STD) between DGS and IGS results was calculated. The STD was generally considered acceptable at $\leq 10\%$. When a $STD > 10\%$ was noted, the results were considered only as estimates of the actual concentration. However, when the chemical results show relatively low values, i.e., ≤ 5 times the detection limit, the STD cannot be significantly evaluated. Quality-Assurance/Quality-Control results indicated STD values within 10%, confirming the replicability of the analyses, while the analytical results were validated by testing the ionic balance, for which values of $\pm 10\%$ were obtained overall.

Determination of salinity classes

To discuss the variations in chemical composition of groundwater in terms of its Cl levels, classes of salinity were determined. The Cl concentrations of the groundwater samples range from 0.003 to 423 meq/L (0.1 to 15,000 mg/L). The inflection points on the cumulative density curve of Cl

concentrations (i.e., plotting the probability of a sample concentration relative to a sample set) are considered to be the thresholds limiting the different salinity classes (Oberhelman and Peterson 2020). Because the present study did not aim to determine salinity classes by distinguishing between aquifer types or even geological provinces, all 2608 groundwater samples were considered in this analysis, regardless of their underlying lithology or aquifer type.

Statistical analysis

Within each salinity class, the concentrations of each chemical constituent are presented in a box-and-whisker diagram (boxplot), which includes the statistical upper quartile (Q₃; 50–75% above the median) and the lower quartile (Q₁; the lowest 25% of numbers), the median, the maximum (elevated), and minimum (lower) concentrations of each chemical constituent. For each of the 12 investigated chemical constituents, the boxplot results—relative to salinity class—are described. Furthermore, the median value of each boxplot is used for determining the trend of the variation in the chemical concentration of groundwater; the Mann–Kendall test (Mann 1945; Kendall 1975), integrated into the XLSTAT software (Addinsoft 2021), was used for this purpose. The null hypothesis (H_0) of the Mann–Kendall test indicates no trend, whereas the alternate hypothesis (H_a) indicates either an upward or a downward trend. A positive Kendall τ corresponds to an upward trend, whereas a negative Kendall τ indicates a downward trend (Pohlert 2020).

Development and validation of the predictive model

We propose a groundwater predictive model able to determine the chemical profile of groundwater. This proposed predictive model may be a helpful tool for homeowners and/or groundwater managers to gain insight into the quality of a groundwater via a simple and direct measurement of its EC. This predictive model can also be used to screen groundwater samples in order to determine which among them may require more comprehensive chemical analyses; such early determination may help avoid unnecessary testing, which tends to be costly and time-consuming. The model achieves this discrimination based on the identification of the salinity class of a groundwater sample. The salinity class for a given groundwater sample can be determined from the direct in-situ measurement of the groundwater EC, using an equation proposed in the present study that establishes a link between the Cl concentration and the EC (EC data is included in the PACES chemical database). The predictive model contains a series of chemical constituents; to each of these corresponds a representative value according to each salinity class. The representative value of each chemical constituent

was established through a boxplot statistical analysis. The median values of the boxplot were adopted for the proposed model, rather than the outlier values, as the median values are more representative of a dataset.

The validation of the proposed predictive model was carried out by comparing the established median value of each of the 12 chemical constituents in the predictive model against equivalent control values drawn from another data source (i.e., other groundwater samples collected during the PACES Program that were not a part of the 2009–2015 PACES data used in the present study but taken from the 2018–2022 PACES Projects). Validation was a three-step process. Firstly, the Cl concentrations in groundwater samples from the control data were determined by using an equation linking the Cl concentration to the EC, which was measured in situ. Secondly, the control groundwater samples were classified and grouped according to their salinity level determined from their calculated Cl concentration. Thirdly, the median value—of each of the 12 chemical constituents—of each determined salinity class (actual value) is compared to the chemical constituent value of the predictive model (predicted value). Here, the correlation between the actual and predicted values is used to judge the predictive model efficiency.

Description of results

Salinity classes

Based on the inflection points in the cumulative density curve of Cl in groundwater, six salinity intervals were initially established (Fig. 2a). However, because the Cl interval from 12.4 to 423 meq/L (i.e., 440 to 15,000 mg/L) was very large in terms of Cl concentration, it was refined by graphically detecting sub-inflection points (Fig. 2b). The inflection points are represented as points connecting different slopes on the cumulative density curve. Thus, a total of eight salinity classes were considered for the present study (Table 1).

Distribution of the chemical constituents within salinity classes

Distribution of major anions

The boxplot statistical distribution of HCO_3^- and SO_4^{2-} concentrations, from the dataset of 2608 groundwater samples, is shown in Figs. 3 a and b, respectively. The median HCO_3^- concentrations overall revealed an increasing trend that was confirmed by a positive Kendall τ_b with p value < 0.05 (see supplementary material). The median HCO_3^- values show an increase starting from 0.9 meq/L (53 mg/L) at salinity class 1 ($\text{Cl} < 0.005$ meq/L) to a value of 6.1 meq/L

(374 mg/L) at salinity class 6 ($\text{Cl} = 12.4\text{--}45.1$ meq/L) (Fig. 3a). However, for $\text{Cl} > 45.1$ meq/L, the median HCO_3^- concentrations show a decrease relative to the increase in Cl concentration (Fig. 3a). In Fig. 3a, the median HCO_3^- concentrations in salinity classes 1–4 ($\text{Cl} < 1.4$ meq/L; i.e., 50 mg/L) are greater than the corresponding Cl concentrations, suggesting a dominance of HCO_3^- in salinity classes 1–4 (dominance of chemical element compared to another one means here that its concentration is greater than that of the compared element). Conversely, for Cl concentrations > 12.4 meq/L (> 440 mg/L) in salinity classes 6–8, the median HCO_3^- concentrations are lower than the corresponding Cl concentrations of classes 6–8. This observation suggests a dominance of Cl for the samples belonging to these classes 6–8. Salinity class 5 ($\text{Cl} = 1.4\text{--}12.4$ meq/L) represents a transition from HCO_3^- -dominant to Cl-dominant; it has a median HCO_3^- concentration of 4.3 meq/L (262 mg/L), which is within the Cl variation interval of salinity class 5 ($\text{Cl} = 1.4\text{--}12.4$ meq/L), confirming a transitional state from HCO_3^- -dominant to Cl-dominant. The interquartile interval of HCO_3^- (i.e., difference between the lower and upper quartiles) progressively increases through salinity classes 1–8 (except class 7), suggesting an increasing variation in HCO_3^- concentration relative to the increase in Cl concentration.

Unlike HCO_3^- , the median SO_4^{2-} concentration (Fig. 3b) consistently increases through the eight salinity classes; this is also confirmed by a positive Kendall τ_b with p value < -0.05 (see supplementary material). The greatest SO_4^{2-} increase between salinity classes was observed between classes 7 ($\text{Cl} = 45.1\text{--}118.5$ meq/L) and 8 ($\text{Cl} > 118.5$ meq/L), with a median SO_4^{2-} concentration increasing from 2.5 meq/L (120 mg/L) to 35 meq/L (1700 mg/L). The SO_4^{2-} interquartile interval (Fig. 3b) progressively increases from salinity class 1 to 8, suggesting that the variability of SO_4^{2-} concentrations is in correlation with the increase in Cl concentrations. In salinity class 8, the maximum/minimum SO_4^{2-} concentrations (i.e., the whisker outlier values) are close to the first and third quartiles (Fig. 3b). This indicates that, despite having the largest interquartile interval, class 8 has a narrow variation of SO_4^{2-} relative to interquartile interval limits. The median SO_4^{2-} concentrations through salinity classes 1–2 are greater than the corresponding Cl concentrations of classes 1–2, suggesting SO_4^{2-} dominance over Cl in salinity classes 1–2 (Fig. 3b). In contrast, for Cl concentrations > 1.4 meq/L (> 50 mg/L), corresponding to salinity classes 5–8, the median SO_4^{2-} concentrations are lower than the corresponding median Cl concentrations. This suggests that Cl is dominant over SO_4^{2-} in salinity classes 5–8. Salinity classes 3 and 4 correspond to median SO_4^{2-} concentrations of 0.2 and 0.4 meq/L, which are within the Cl variation interval of salinity classes 3 ($\text{Cl} = 0.02\text{--}0.3$ meq/L) and 4 ($\text{Cl} = 0.3\text{--}1.4$ meq/L). For this reason, salinity classes 3 and 4 may be considered as

Fig. 2 Cumulative density curves for the Cl concentration in groundwater. In (a), the data are expressed by log scale because the interval of cumulative density values is too large from 0.00001 to 100; whereas in (b), the data are expressed by a linear scale as the cumulative density is small (from 30 to 100) compared to that illustrated in (a)

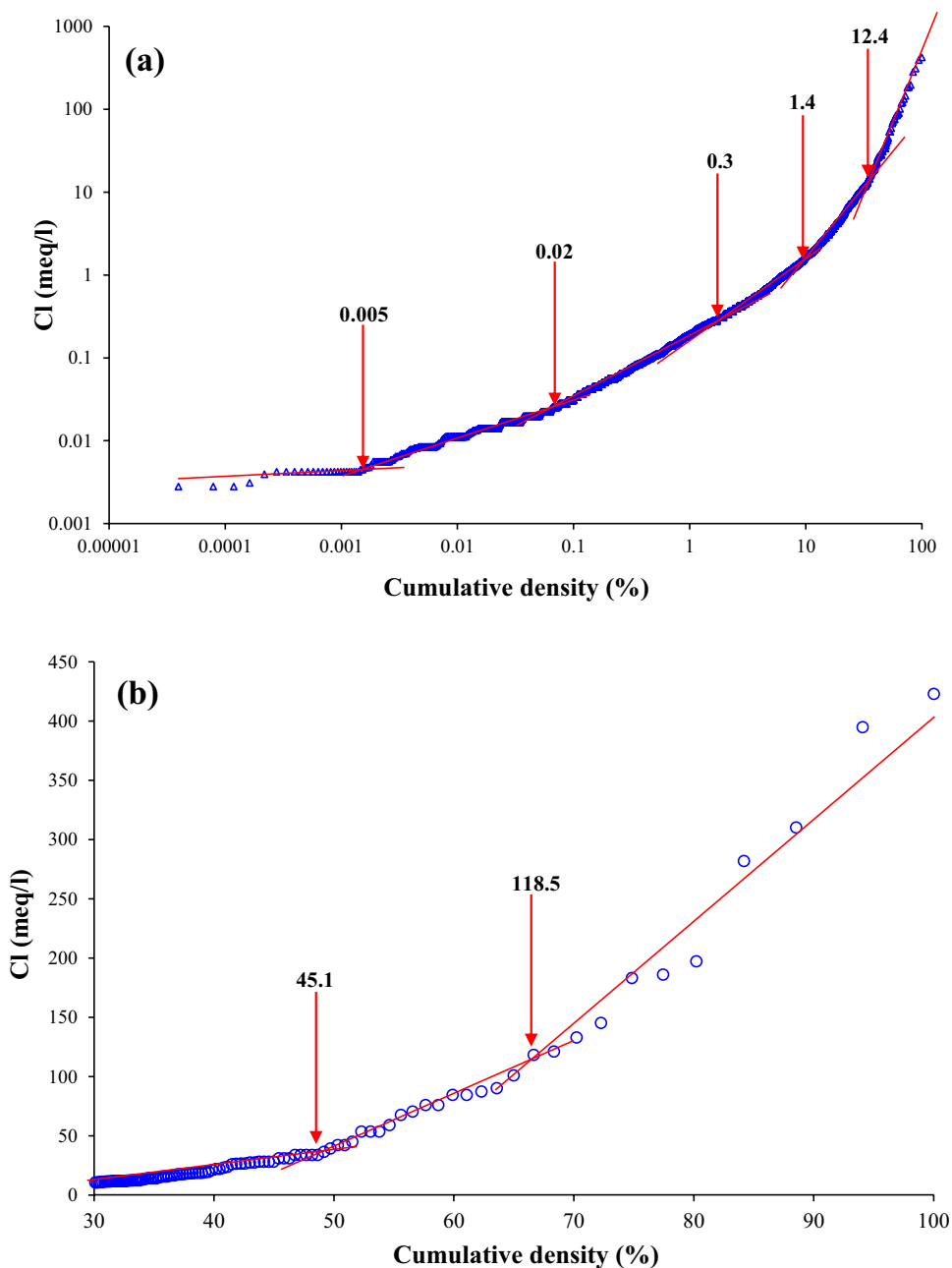


Table 1 Thresholds of salinity classes of the PACES dataset

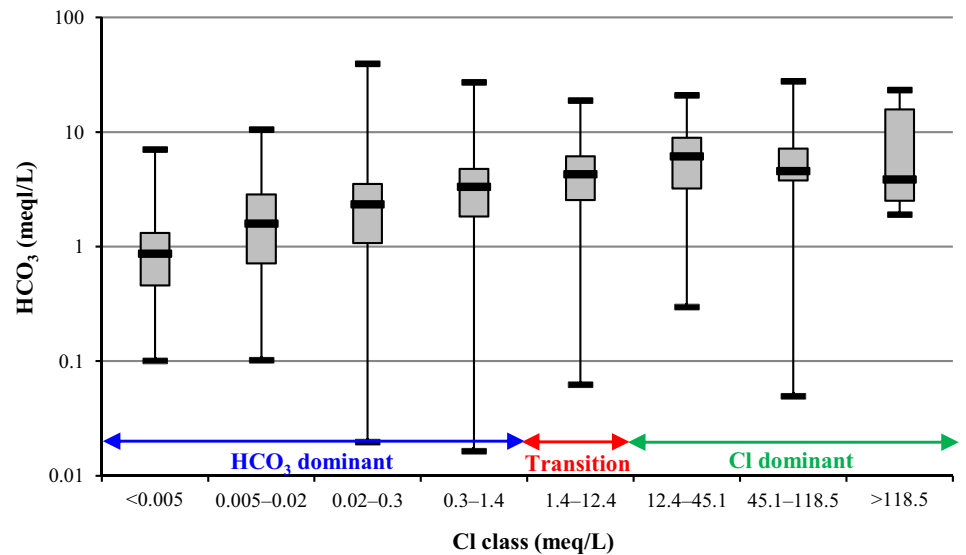
Salinity class	Interval (meq/L)	Interval (mg/L)	Samples (<i>n</i>)
1	<0.005	<0.16	25
2	0.005–0.02	0.16–0.8	260
3	0.02–0.3	0.8–10	978
4	0.3–1.4	10–50	775
5	1.4–12.4	50–440	429
6	12.4–45.1	440–1,600	57
7	45.1–118.5	1,600–4,200	14
8	> 118.5	> 4,200	11

transitional between groundwater dominated by SO₄ to groundwater dominated by Cl.

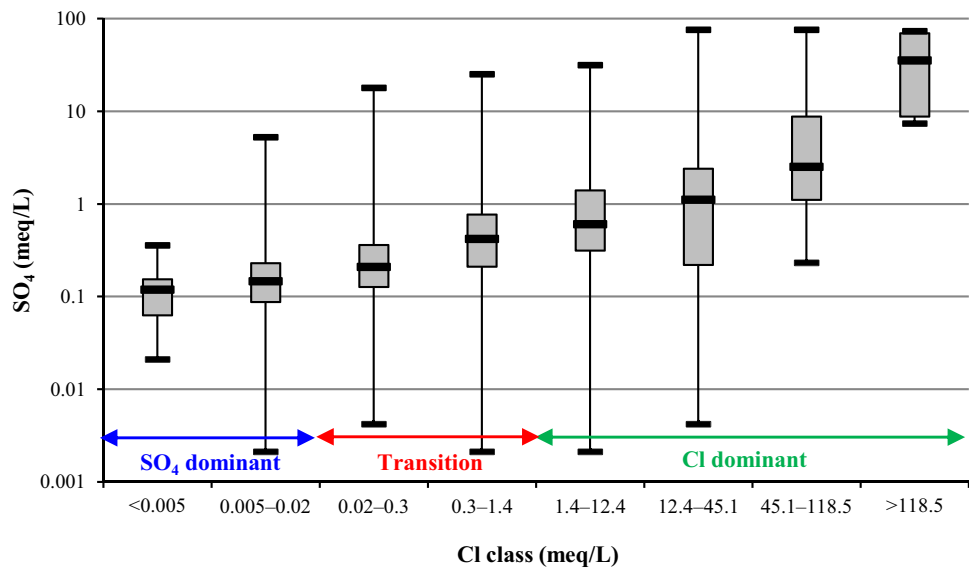
Distribution of major cations

Figures 4a–d show that the concentrations of each of the major cations increase as Cl concentration increases; an observation confirmed with a positive Kendall τ (see supplementary material). In Fig. 4a, groundwater samples through salinity classes 1–4 are dominated by Ca, as Ca median values (0.8, 1, 1.5, and 2 meq/L) are greater than the Cl concentration corresponding to salinity classes 1–4.

Fig. 3 Boxplot distribution of major anions over the Cl classes: **a** HCO_3^- and **b** SO_4^{2-}



(a)



(b)

Inversely, classes 6–8 are found to be dominated by Cl. Salinity class 5 corresponds to a median Ca concentration of 2.3 meq/L, which is within the Cl variation interval of salinity class 5 ($\text{Cl}=1.4\text{--}12.4$ mg/L). Hence, salinity class 5 corresponds to a transition between groundwater dominated by Ca to groundwater dominated by Cl. The median Mg values (Fig. 4b) are observed to overlap the Cl concentration in salinity classes 1–3; therefore, there is a tendency for dominance of magnesian water types in these salinity classes 1–3. Salinity class 4 corresponds to a median Mg concentration of 0.7 meq/L, which is within the Cl variation interval of salinity class 4 ($\text{Cl}=0.3\text{--}1.4$ meq/L). This suggests that salinity class 4 also represents a transition. Indeed, Cl concentrations in classes 5–8 are greater than the

corresponding median Mg concentrations, suggesting, in this case, the dominance of Cl over Mg.

The median K values (Fig. 4d) show that groundwater samples in salinity classes 1–2 are dominated by potassic water type, as K median values are greater than Cl concentration, corresponding to salinity classes 1–2. Inversely, classes 4–8 have Cl concentrations greater than K concentrations, suggesting Cl water type dominance across these classes. Salinity class 3 corresponds to a median K concentration of 0.04 meq/L, which is within the Cl variation interval of salinity class 3 ($\text{Cl}=0.02\text{--}0.3$ mg/L); therefore, salinity class 3 corresponds to a transition between groundwater dominated by K to groundwater dominated by Cl. In Fig. 4c, the median Na concentrations through classes

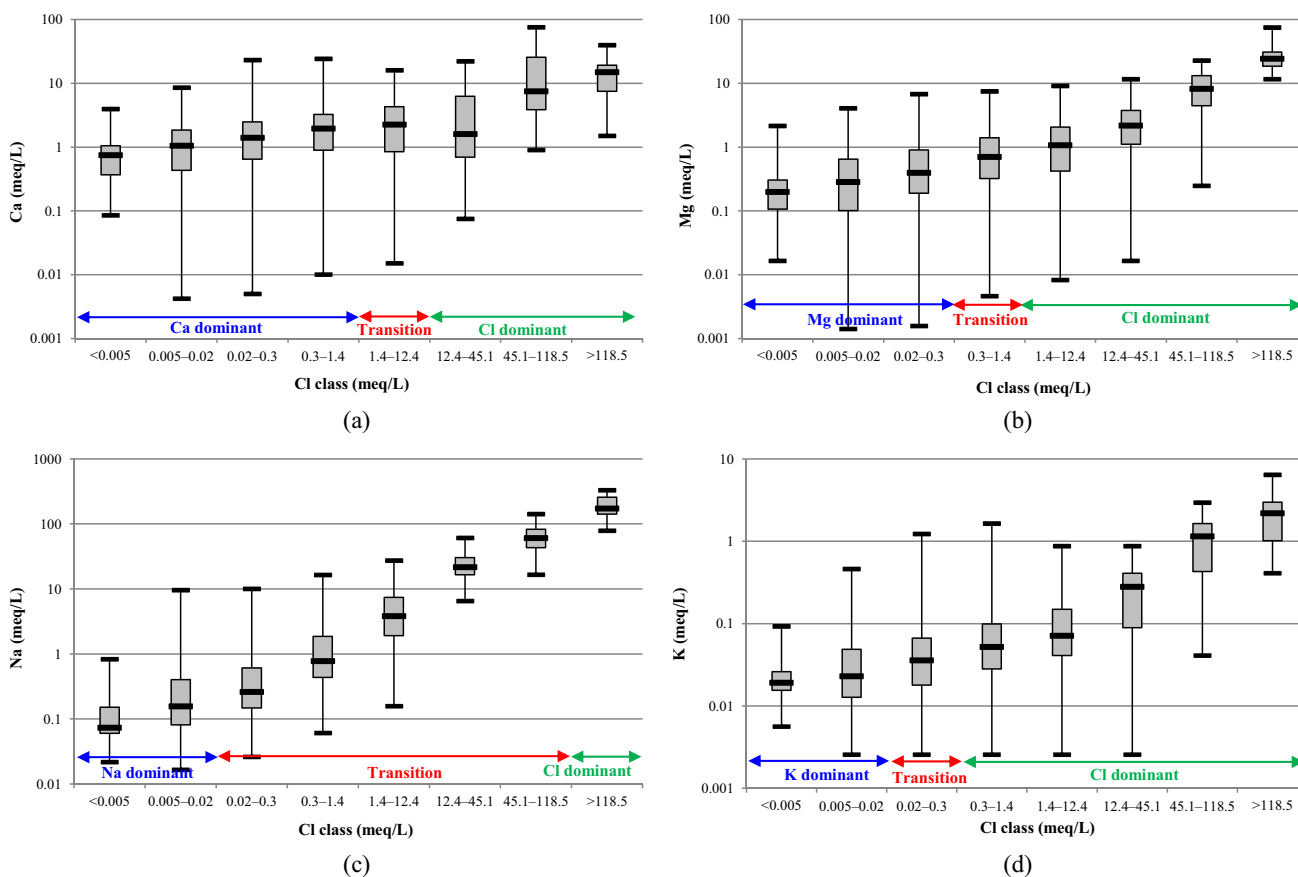


Fig. 4 Boxplot distribution of major cations over the Cl classes: **a** Ca, **b** Mg, **c** Na, and **d** K

1 ($Na = 0.07$ meq/L) and 2 ($Na = 0.16$ meq/L) are found to be greater than the corresponding Cl concentrations of classes 1 ($Cl < 0.005$ meq/L) and 2 ($Cl = 0.005-0.02$ meq/L), respectively. Hence, Na is dominant over classes 1–2. For Cl concentrations > 118.5 meq/L (class 8), the median Na concentration (173.3 meq/L) is greater than 118.5 meq/L. However, this does not indicate that Na is dominant with respect to Cl, as class 8 includes Cl concentrations even greater than 173.3 meq/L, and appropriately suggests that Cl is dominant over Na in this salinity class 8. Classes 3–7 correspond to median Na concentrations that are within the Cl variation interval of the corresponding salinity classes. Hence, classes 3–7 constitute a transition from groundwater dominated by Na to groundwater dominated by Cl.

In this study, median Ca concentrations (Fig. 4a) are observed to be higher than median Na concentrations (Fig. 4c) for Cl concentrations < 1.4 meq/L (< 50 mg/L), i.e., over classes 1–4. For $Cl > 1.4$ meq/L (i.e., over classes 5–8), Na concentrations become inversely dominant over Ca. The median Ca concentration corresponding to salinity class 6 (1.6 meq/L) was found to be slightly lower than that of the preceding class 5 (2.3 meq/L). The Na concentrations over classes 5–6 increase substantially from 3.8 to 21.8 meq/L.

As Na concentrations are dominant over Ca concentrations in the highest salinity classes (classes 5–8), groundwater samples having the highest salinity are generally of the Na-Cl water type.

Distribution of minor elements B, Ba, Sr, and Si

The boxplot statistical distributions of the four minor elements B, Ba, Sr, and Si, relative to the Cl concentration (in mg/L), are shown in Fig. 5a–d, respectively. Boron, Ba, and Sr concentrations generally increase as the Cl concentration increases. This observation is confirmed through the positive Kendall τ presented in the supplementary material. Strontium shows the most pronounced increase in concentration, with median values ranging from 0.04 (salinity class 1: $Cl < 0.16$ mg/L) to 18 mg/L (class 8: $Cl > 4200$ mg/L). It appears that relative to the increase in Cl, there is a no regular enrichment of Ba and B compared to Sr. The median Ba concentrations in salinity classes 1–5 (median Ba = 0.007, 0.016, 0.04, 0.07, and 0.1 mg/L) are comparable to median B concentrations in each corresponding class (median B = 0.007, 0.014, 0.03, 0.04, and 0.1 mg/L). In salinity classes 6–7 (Cl 440–4200 mg/L), median B concentrations

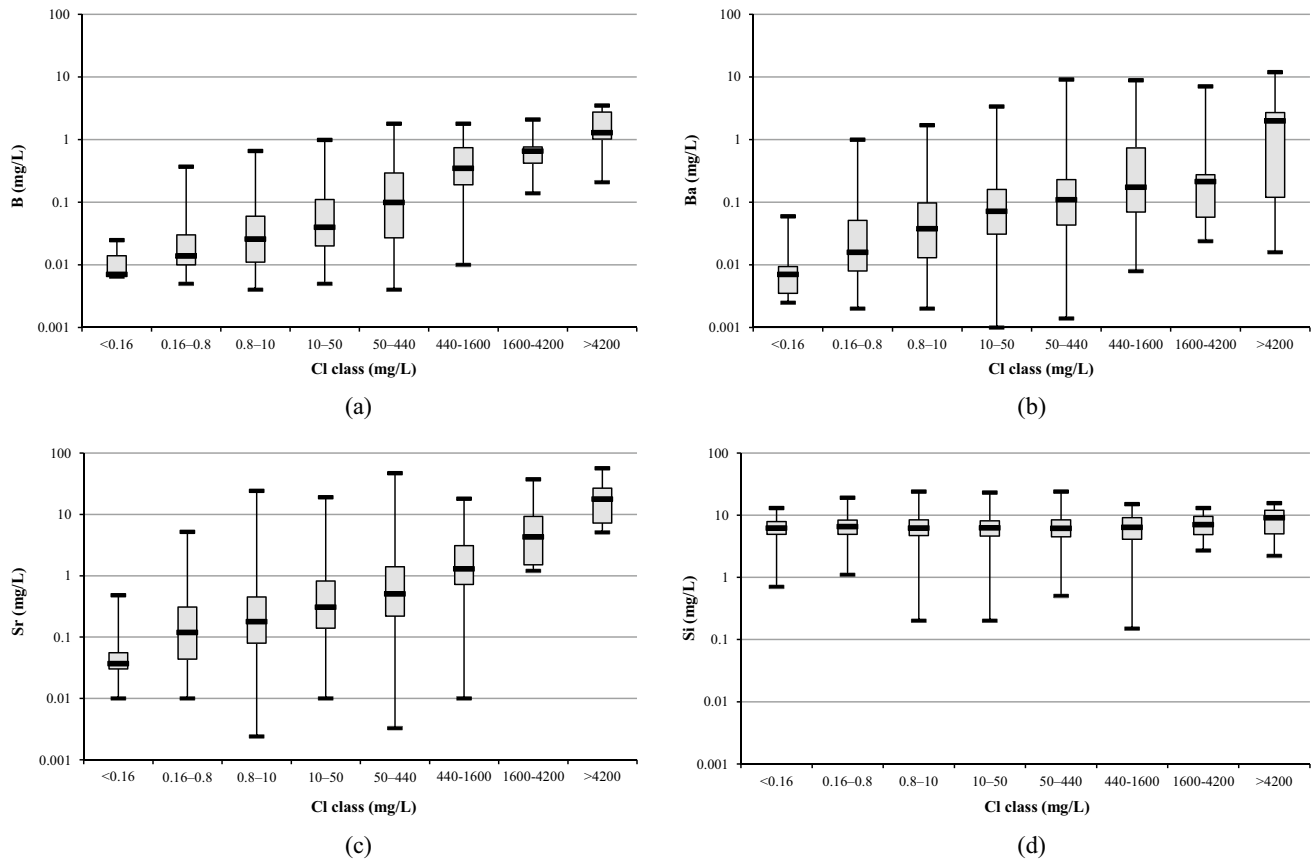


Fig. 5 Boxplot distribution of minor elements over the Cl classes: **a** B, **b** Ba, **c** Sr, **d** Si

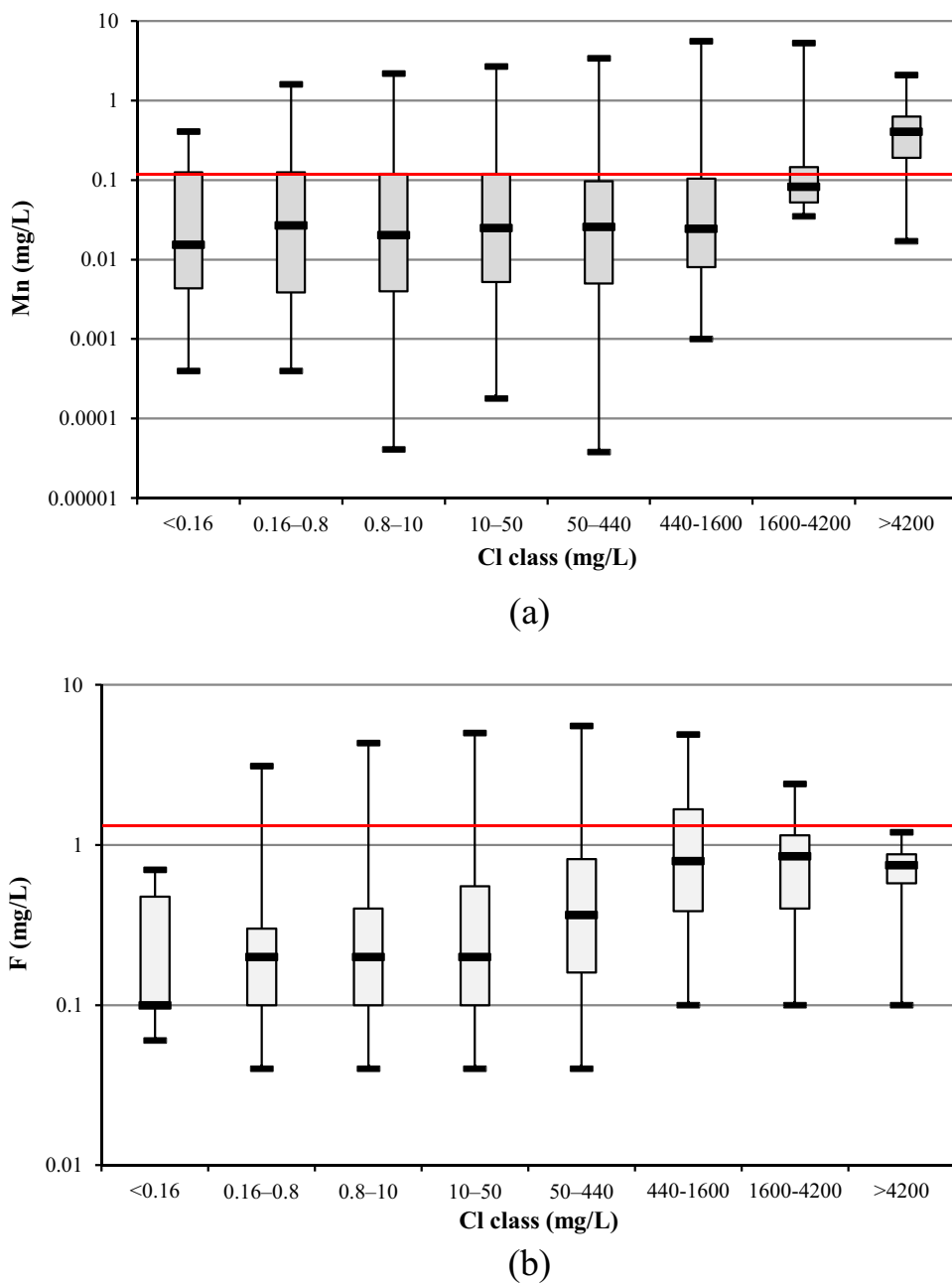
(median B = 0.35 and 0.66 mg/L) are higher than Ba (median Ba = 0.18 and 0.22 mg/L). For the highest Cl concentration class (class 8: Cl > 4200 mg/L), the median Ba concentration (2 mg/L) is found to be higher than the B concentration (1.3 mg/L). Also, the maximum Ba concentration (12 mg/L) is observed to be significantly higher than the maximum B concentration (3.5 mg/L). B is dominant over Ba in groundwater samples having a Cl concentration ranging from 440 to 4200 mg/L, whereas Ba becomes dominant over B when the Cl concentration in groundwater is > 4200 mg/L. Through salinity classes 1–7, the median Si concentrations show a very slight variation ranging from 6 to 9 mg/L (Fig. 5d), suggesting that Si has limited sensitivity to salinity variation. Indeed, the Mann-Kandel result related to Si (see supplementary material) indicates that the Si trend is not statistically significant with a p value of 0.105 greater than the confidence level of 0.05.

Distribution of trace elements Mn and F

Two trace chemical elements are considered in the present study, Mn and F, because elevated concentrations of these elements in groundwater can exert a significant impact on

the quality and drinkability of groundwater with regards to human health. In several studies conducted in Southern Quebec, concentrations of Mn and F in groundwater have exceeded Canadian standards for drinking water (acceptable limits are Mn = 0.12 mg/L; F = 1.5 mg/L) (Montcoudiol et al. 2015; Saby et al. 2016; Walter et al. 2017; Bondu et al. 2020; Health Canada 2020). In this study, the median Mn concentrations are lower than 0.1 mg/L for groundwater Cl concentrations < 4200 mg/L (classes 1–7), and the lowest/highest Mn median concentrations are observed for the lowest/highest Cl concentrations (Fig. 6a). The median Mn concentration is observed to be generally constant (0.02 mg/L) over salinity classes 1–6, while in classes 7–8, median Mn concentrations increase to reach a value of 0.4 mg/L. The increase in Mn concentration is mostly limited to high Cl concentrations, which may explain the modest trend of Mn concentrations with p value of 0.048 (see supplementary material). For Cl concentrations < 50 mg/L (classes 1–4), the Mn concentration of groundwater samples in the 3rd quartile (Fig. 6a) is above the maximum acceptable level of Mn in drinking water (0.12 mg/L), whereas the 1st quartile groundwater samples have Mn concentrations below the

Fig. 6 Boxplot distribution of trace elements **a** Mn and **b** F in the Cl classes. The red line indicates the maximum acceptable concentrations of these elements in Canadian drinking water



acceptable limit (Fig. 6a). Median F concentrations range from 0.1–0.8 mg/L, and do not exceed 1 mg/L through all salinity classes (Fig. 6b). Median F concentrations over salinity classes 1–4 (Cl = 0.16–50 mg/L) do not show significant variation, with a value of 0.2 mg/L. Subsequently, the median F concentrations increase as Cl concentrations increase, reaching a value of 0.8 mg/L in saline class 8 (Cl > 4200 mg/L), justifying the positive F-Kendall τ_b with a *p* value < 0.05 (see supplementary material). In Fig. 6b, the 3rd quartile groundwater samples show F concentrations below the Canadian drinking water standard of 1.5 mg/L through all the salinity classes, except salinity

class 6 (Cl = 440–1600 mg/L) for which the 1st quartile groundwater samples are below the standard of 1.5 mg/L.

Presentation and validation of the proposed empirical predictive model

To propose an empirical predictive model of the concentrations of the chemical constituents in groundwater relative to the concentrations of Cl, the median values (expressed in mg/L) of the 12 chemical constituents investigated in this study were considered. Table 2 summarizes the median

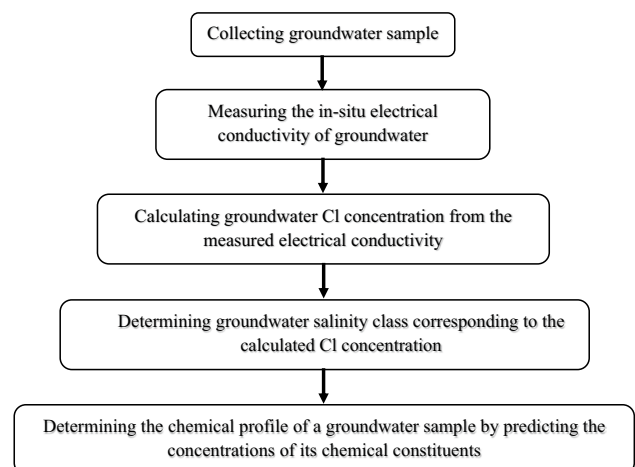
Table 2 Predictive model to determine groundwater chemical profile based on salinity level: correlation between the salinity levels of groundwater and the concentrations of 12 chemical constituents (developed using the 2009–2015 PACES Program data)

Group	Element	Stand. *	Salinity class							
			1	2	3	4	5	6	7	8
			Cl concentration (mg/L)							
			< 0.16	0.16–0.8	0.8–10	10–50	50–440	440–1600	1600–4200	> 4200
Anions	HCO ₃	200	53	95	134	202	261	374	278	235
	SO ₄	200	6	7	10	20	29	50	120	1700
Cations	Ca	75	15	21	28	39	45	32	135	300
	Mg	30	2	3	5	9	13	27	100	294
	Na	200	2	4	6	18	88	500	1400	3981
	K	12	0.75	0.90	1.40	2.05	2.80	11	45	85
Minor and trace elements	B	5	0.007	0.014	0.025	0.04	0.1	0.35	0.66	1.3
	Ba	1	0.007	0.016	0.038	0.072	0.11	0.18	0.22	2
	Sr	7	0.04	0.12	0.18	0.31	0.51	1.3	4.3	17.8
	Si	–	6.2	6.6	6.2	6.3	6.2	6.4	7.05	9.15
	Mn	0.12	0.0155	0.025	0.019	0.024	0.026	0.025	0.083	0.41
	F	1.5	0.1	0.2	0.2	0.2	0.4	0.8	0.8	0.7

*Drinking water limit concentration in mg/L (WHO 2017; Government of Canada 2021)

concentrations of these chemical constituents relative to the Cl concentration expressed in mg/L (salinity classes). Table 2 constitutes the predictive model that makes it possible to determine the chemical profile of groundwater relative to the Cl level. This predictive model is proposed to help homeowners/groundwater managers gain valuable insight regarding groundwater quality prior to costly laboratory analyses. To apply the predictive model to a given groundwater sample, the methodology, first, consists of determining the EC of the groundwater sample; this is easily done in situ in the field. Secondly, based on the value of the groundwater EC, calculate the value of groundwater Cl concentration using an equation linking Cl to EC. Equations linking Cl to EC have been proposed in the literature (e.g., Howard and Haynes 1993; Meriano 2007). Following a similar approach, the best relationship according to the Southern Quebec groundwater database employed in this study is $Cl = 0.0047 \times EC^{1.4273}$ (equation developed based on the fitted linear relationship of Cl in mg/L with EC in $\mu S/cm$). Once the Cl concentration of groundwater sample is calculated from the EC, thirdly, the use of Table 2 allows to determine the salinity class, corresponding to the determined Cl concentration, to which a groundwater sample belongs. Knowing the salinity class makes it possible to determine the chemical profile of a groundwater sample by predicting the relative concentrations of the chemical constituents. Figure 7 summarizes the successive steps of the proposed survey methodology approach. In certain situations, this model may provide preliminary information on groundwater that either makes it possible to avoid resorting to laboratory

chemical analyses, or on the contrary, indicates the need to proceed with further analyses. The predictive model proposed in the present study was developed using data drawn from the PACES groundwater chemistry and may, therefore, be appropriately applied to the regions of Southern Quebec. However, the methodology used to develop this predictive model may be applied to datasets drawn from other groundwater databases, to predict groundwater chemical profile in other regions. In the present study, the groundwater predictive model is limited to 12 inorganic chemical constituents (HCO₃, SO₄, Ca, Mg, Na, K, Ba, B, Sr, Si, Mn, and

**Fig. 7** Successive steps of the proposed survey methodology approach

F), but can be extended in other studies to other chemical constituents.

The validation of the predictive model (Table 2) was undertaken by applying the established salinity classes to an independent dataset. The objective of the validation was to verify whether the concentrations predicted by the model for a given groundwater samples match the actual concentrations that were measured. For this purpose, we used the results of an independent chemical analysis of 313 groundwater samples drawn from a different dataset than the dataset used to develop the predictive model. These independent groundwater samples were collected from the Mauricie-2 and Lanaudière regions belonging to Southern Quebec (Tremblay et al. 2021) and analyzed for different inorganic constituents including the 12 elements: Ca, Mg, Na, K, HCO₃, SO₄, B, Sr, Mn, Ba, Si, and F. The validation approach started by categorizing the 313 groundwater samples according to their Cl concentration into one of the 8 predetermined salinity classes indicated in Table 1. The

Cl concentrations of these independent groundwater samples ranged from 0.17 to 2200 mg/L, and they were accordingly classified as follows: class 2: *n* = 53; class 3: *n* = 96; class 4: *n* = 92; class 5: *n* = 63; class 6: *n* = 9, class 7: *n* = 1; class 8: *n* = 1 (there was no sample in class 1). As classes 7 and 8 contained only one value, they were excluded from the validation process. For groundwater samples in each of the 5 retained salinity classes (2–6), the median of each chemical constituent was calculated (measured concentration) and correlated to the predicted concentrations presented in Table 2. The relationship between the measured and predicted concentrations in Fig. 8 showed a strong correlation coefficient (*R* = 0.95; *p* value < 0.05 according to the Kendall statistical test). This high level of correlation indicates that the proposed predictive model was able to consistently predict the approximate concentrations, i.e., the chemical profile of all 12 of the studied chemical constituents.

Discussion

Table 3 summarizes the distribution of dominant chemical elements within each salinity class. This table shows the transitions identified between the dominant chemical elements relative to Cl, as are the variable salinities at which major elements are dominant. In the present study, the distribution of chemical elements throughout the 8 salinity classes is further distinguished by comparing the dominant elements in the salinity classes using a Piper plot. Mg and K transitions are found in the moderate salinity classes 3 and 4, respectively (Table 3), but given the high Mg concentration over K concentration (10–15 times in meq/L), magnesium salt is dominant over potassium salt. However, Mg-Cl is not expected to be the dominant water type as the Piper diagram (Fig. 9) shows that most groundwater samples from classes 6–8, with 25% of samples from class 5, are dominated by Na-Cl water type, explained by the abundance of Na over Mg concentration. The transition, from Na dominant to

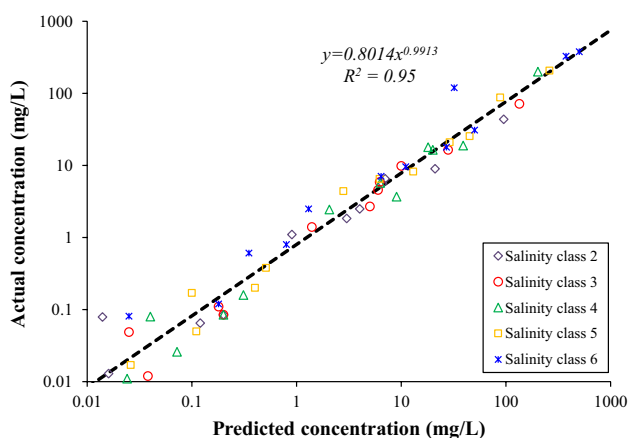


Fig. 8 Correlation between the predicted and measured concentrations (the 60 points in this figure represent 12 chemical constituents over 5 salinity classes of 313 groundwater samples)

Table 3 Distribution of dominant chemical elements in the 8 salinity classes

	Salinity class								
	1	2	3	4	5	6	7	8	
	Dominant water type* with % of groundwater samples								
	Ca-HCO ₃ (100%)	Ca-HCO ₃ (90%)	Ca-HCO ₃ (87%)	Ca-HCO ₃ (73%)	Ca-HCO ₃ (38%) Na-Cl (26%)	Na-Cl (87%)	Na-Cl (85%)	Na-Cl (100%)	
Ca									
HCO ₃									
K									
SO ₄									
Mg									
Na									

■ Anion/cation-dominant ■ Transition ■ Cl-dominant

* Dominant water types are identified from Figure 7

*Dominant water types are identified from Figure 7

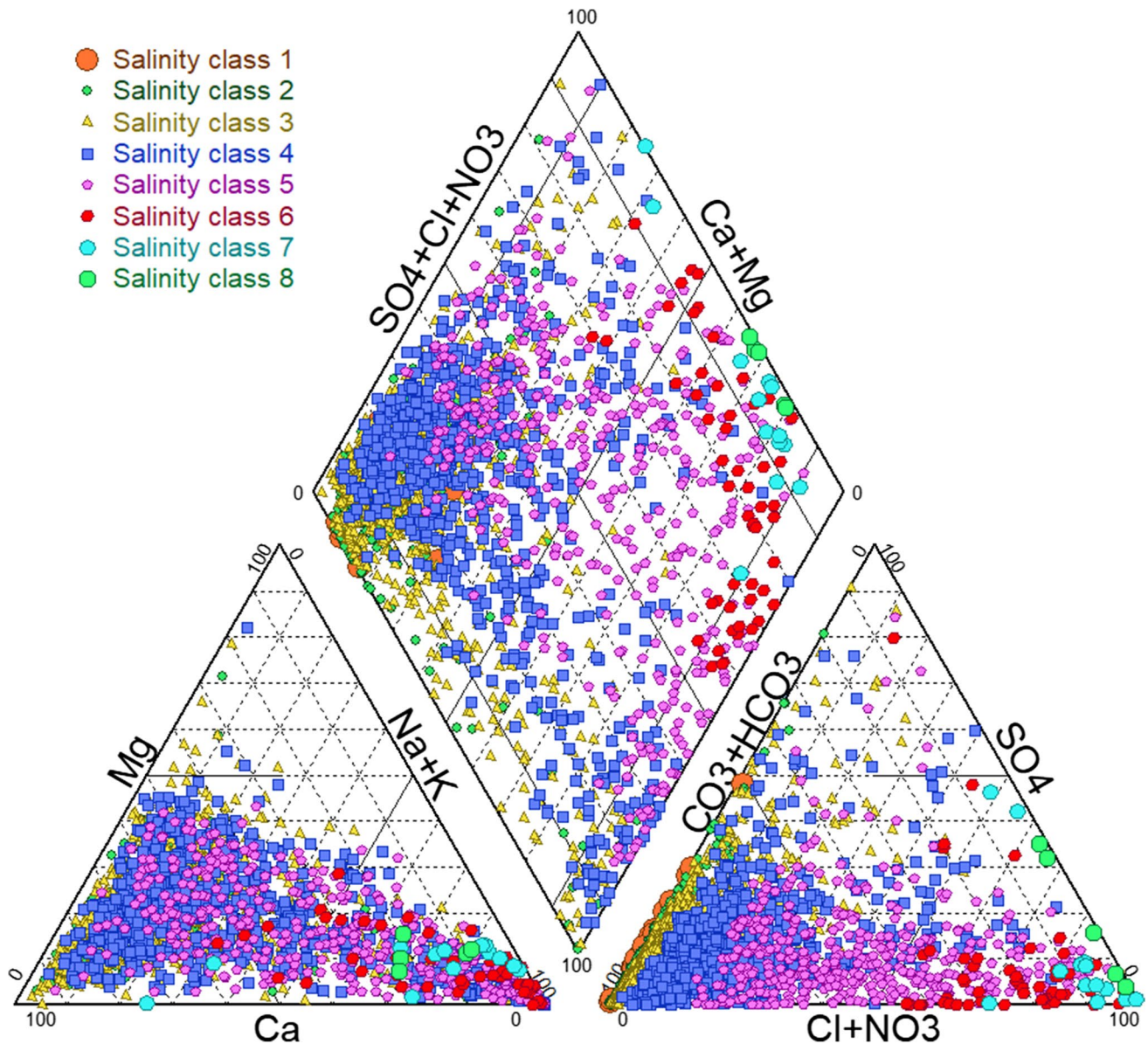


Fig. 9 Piper plot of groundwater samples by distinguishing their salinity classes

Cl dominant groundwater, was observed over classes 3–7 (Table 3). The Piper plot (Fig. 9) shows that samples from this transition distinguish two main water types. Here, 87% of samples from class 3 and 73% of samples from class 4 are overall dominated by a Ca-HCO₃ water type, whereas most samples from classes 6 (87%) and 7 (85%), as well as 25% from class 5, are generally dominated by a Na-Cl water type (Fig. 9). The presence of a Ca-HCO₃ water type within this transition is related to the high concentration of Ca compared to Na in classes 3 and 4. In classes 5, 6, and 7, the dominance of Na concentration over Ca concentration explains the occurrence of a Na-Cl water type. Identifying class 5 as transition from HCO₃ and Ca dominant to Cl

dominant appears to be logical, as the preceding classes 1–4 are dominated by a Ca-HCO₃ water type, whereas classes 6–8 are dominated by a Na-Cl water type (Fig. 9).

An increase of the concentrations of the major elements (HCO₃, SO₄, Ca, Mg, Na, and K) and some minor chemical constituents (Ba, B, and Sr) relative to the increase in Cl concentration is observed in the PACES data. Similarly, Mora et al. (2020), who studied the dynamics of major and trace elements along the groundwater flow path of the sedimentary Todos Santos aquifer in Baja California Sur (Mexico), found that the major and minor elements exhibited increasing trends relative to the increase in Cl concentration. The results from the present study—showing that

major elements, relative to the increase of Cl, were found to be dominant in the lower salinity classes, whereas the Cl becomes dominant in the highest salinity classes—are also consistent with the observations of Hanor (1994), who underlined that lower-salinity water often contains HCO_3 and SO_4 as dominant anions, whereas Cl makes up over 95% by mass of the anions in groundwater exhibiting a salinity greater than 10,000 mg/L. In the present study, as observed in the Todos Santos aquifer by Mora et al. (2020), the minor elements Si and F vary conservatively relative to the increase in Cl concentration. Cation exchange processes appeared to be responsible for the increase in Na and K relative to the increase in Cl concentrations in Todos Santos, whereas the increases in HCO_3 , SO_4 , and B were associated with the release of these elements due to carbonate mineral weathering (Mora et al. 2020). Numerous experimental studies have led to the understanding that certain geochemical processes govern the concentrations of chemical elements in groundwater relative to the increase in Cl concentration (Amrhein et al. 1992; Paalman et al. 1994; Sun et al. 2015). In the present study, the transition from Ca-dominant water to Cl-dominant water was observed at salinity class 5, i.e., in water that exhibits a Cl concentration of approximately 1.4–12.4 meq/L (10–50 mg/L). The decrease in Ca concentrations in salinity classes 5–6 suggests the involvement of high Cl concentration in causing the Ca- HCO_3 -dominant groundwater to become Na-Cl-dominant groundwater (Moore et al. 2017). Such a process will lead to a decrease in Ca concentration. However, the high concentrations of Ca observed in classes 7–8, compared to the other salinity classes 1–6, can also result from incongruent weathering reactions (Wigley 1973). Like Ca, the other chemical constituents such as B, Ba, Sr, and Mg may also increase in concentration in groundwater during cation exchange (Charette and Sholkovitz 2006; Mahlkecht et al. 2017). Silica in groundwater is exclusively derived from water–rock interaction; the groundwater dissolves the silica through weathering of silicate minerals in rocks and sediments (Khan et al. 2015). The most common Si-bearing minerals are plagioclase, feldspars, and quartz (Miretzky and Alicia Fernández 2004). Analysis of cuttings from drilling wells in the study area shows that silicate rocks (e.g., granite and gneiss) are rich in plagioclase-feldspar minerals (Montcoudiol et al. 2015). This suggests initially that Si-groundwater in the study area may have originated from the weathering of silicate rocks. However, over the study area, Si concentrations in groundwater were found to be limited to a maximum of 24 mg/L; this relatively low concentration (1–30 mg/L) implies less water–rock interaction (Khan and Umar 2010). Silica can exist in solution as chemically unreactive stable species, usually showing no affinity for other major dissolved constituents (Haines and Lloyd 1985). This may explain why, through salinity classes 1–7 in the present study, the median Si concentrations show

a very slight variation ranging from 6 to 9 mg/L. Strontium is a common trace element in most rocks and can be released into groundwater through the weathering process as well as through the dissolution process, given its high solubility (Luczaj and Masarik 2015; Middelburg et al. 1988; Moldovanyi et al. 1990). Strontium concentrations are generally low in ultrabasic rocks and sandstones, but high concentrations have been found in carbonate rocks (~600 ppm), evaporite media such as gypsum and anhydrite (~3500 ppm), crystalline structures of feldspar plagioclase minerals and carbonate fossils (~10,000 ppm) (Beaucaire and Michard 1982; Franklyn et al. 1991; Kinsman 1969). It is noteworthy that rocks of the study area may contain high concentrations of Sr that contribute Sr to groundwater over all salinity levels. Nonetheless, the observed increase in Sr concentration, relative to the increase of Cl, is significantly higher than would be expected if weathering and/or dissolution processes were the only sources of Sr. The increase in Sr relative to the increase in salinity may therefore also be linked to other mechanisms occurring simultaneously. Sr can occur in combination with Ca and Ba minerals, while Ba-rich groundwater generally contains significant concentrations of Sr (Bondu et al. 2020). On the other hand, Sr can have several anthropogenic sources such as glass products (e.g., ceramics), fly ash from industrial waste coal burning, landfill leachate, and carbonate or phosphate fertilizers (Musgrove 2021). Other geochemical processes such as sorption/desorption, co-precipitation of minerals and mineral dissolution can also take place during the increase in salinity, by involving an increasing/decreasing fraction of the concentrations in major, minor and trace elements (Rusak et al. 2016).

Conclusion

The present study provides a quantitative portrait of the variation in the concentrations of certain chemical constituents in groundwater relative to the salinity level in Southern Quebec aquifers (Canada). It also proposes a predictive model to determine the chemical profile of groundwater based on the Cl concentration level. This study makes use of a groundwater chemistry database containing data drawn from 2608 groundwater samples from 16 Southern Quebec regions covering a total surface area of approximately 100,000 km². The groundwater samples were collected from private, municipal, and observation wells installed both in bedrock and unconsolidated aquifers. This study considers 12 selected inorganic chemical constituents including major, minor, and trace elements (i.e., HCO_3 , SO_4 , Ca, Mg, Na, K, Ba, B, Sr, Si, Mn, and F). Based on the cumulative density curve of Cl concentrations in the groundwater samples, eight salinity classes were established. Graphical analyses were

then applied to document the variations in the concentrations of these chemical constituents throughout the established salinity classes. The results show that the concentrations of chemical constituents increase as the Cl concentration increases; this finding is consistent with those of other studies undertaken elsewhere under different contexts. On the other hand, results show that the salinity of these groundwaters is largely controlled by Cl concentrations, although at low salinity, all of the major elements are important contributors. Concentrations of Ba, B, and Sr increase with increasing Cl concentrations, whereas Si exhibits only limited increases in concentration with increasing salinity. The highest Mn and F concentrations are associated with the highest Cl concentrations. High concentrations of Mn and F, which in many cases exceed regulatory limits, constitute a serious issue in the management of drinking water quality in Southern Quebec's aquifers. Determining the origin of salinity over the study area is beyond the scope of the present study. However, given the observed increase of concentrations of chemical constituents relative to the increase of salinity, effective and sustainable groundwater resources management over the study area may depend on strategies that include the identification of the origins of groundwater salinity. Further studies investigating the sources of groundwater salinity at a regional scale are encouraged.

A predictive model of the major, minor, and trace groundwater chemical constituents, relative to the Cl level, is proposed to help homeowners/groundwater managers gain valuable insight in regard to groundwater quality prior to costly laboratory analyses. The proposed predictive model was based on the 2009–2015 PACES groundwater chemistry data covering the regions of Southern Quebec, wherein the correlation between EC and Cl was identified as follows: $Cl = 0.0047 \times EC^{1.4273}$. The model could be further refined, and the uncertainty reduced by developing knowledge of the geochemical relationships within individual geologic regions, if necessary. The methodology established here for elaborating the predictive model in the present study could be adapted readily to other groundwater chemistry databases in other regions around the world. In the present study, an empirical predictive model of groundwater quality is proposed to determine the chemical profile of a groundwater by predicting the relative concentrations of a set of chemical constituents. This study was limited to 12 inorganic chemical constituents, including some major elements as well as some minor and trace elements. However, it should be noted that a comprehensive prediction of groundwater quality would require the consideration of additional complementary chemical constituents of groundwater, in particular those that have severe adverse health effects. This study was based on the PACES groundwater chemistry database, which is comprised of data drawn from 2608 groundwater samples collected in sixteen regions of Southern Quebec.

The sixteen regions selected for PACES comprise the more densely inhabited regions of the province of Quebec. Consequently, complementary groundwater chemistry data drawn from other Southern Quebec regions would be valuable for future similar studies.

Supplementary Information The online version contains supplementary material available at <https://doi.org/10.1007/s11356-022-19854-z>.

Acknowledgements The authors would like to thank the Quebec Ministry of the Environment (*Ministère de l'Environnement et de la Lutte contre les Changements Climatiques*) that funded this project through the Groundwater Knowledge Acquisition Program (*Programme d'acquisition de connaissances sur les eaux souterraines—PACES*). The authors would like to thank two anonymous reviewers for their valuable comments and suggestions on improving this manuscript.

Author contribution The first draft of the manuscript was written by Dr. Lamine Boumaiza and all authors (Julien Walter, Romain Chesnaux, Randy L. Stotler, Tao Wen, Karen H. Johannesson, Karthikeyan Brindha, and Frédéric Huneau) commented on previous versions of the manuscript. All authors read and approved the final version of the manuscript.

Funding This project is funded by the Quebec Ministry of the Environment (*Ministère de l'Environnement et de la Lutte contre les Changements Climatiques*) through the Groundwater Knowledge Acquisition Program (*Programme d'acquisition de connaissances sur les eaux souterraines—PACES*).

Data availability The data that supports the findings of the study are illustrated in the Figs. 2, 3, 4, 5 and 6 of the present manuscript.

Declarations

Ethics approval Not applicable.

Consent to participate Not applicable.

Consent for publication Not applicable.

Competing interests The authors declare no competing interests.

References

- Addinsoft (2021) XLSTAT statistical and data analysis solution. New York, USA. <https://www.xlstat.com>
- Amrhein C, Strong JE, Mosher PA (1992) Effect of de-icing salts on metal and organic matter mobilization in roadside soils. *Environ Sci Technol* 26:703–709
- ATSDR (Agency for Toxic Substances and Disease Registry) (2010) Toxicological profile for Boron. Department of Health and Human Services, Public Health Service, Atlanta, GA, U.S
- Avrahamov N, Antler G, Yechieli Y et al (2014) Anaerobic oxidation of methane by sulfate in hypersaline groundwater of the Dead Sea aquifer. *Geobiology* 12:511–528
- Barbieri M, Ricolfi L, Vitale S, Muteto PV (2019) Assessment of groundwater quality in the buffer zone of Limpopo National Park, Gaza Province, Southern Mozambique. *Environ Sci Pollut Res* 26:62–77

- Beaucaire C, Michard G (1982) Origin of dissolved minor elements (Li, Rb, Sr, Ba) in superficial waters in a granitic area. *Appl Geochemistry* 16:247–258
- Beaudry C (2013) Hydrogéochimie de l'aquifère rocheux régional en Montérégie est, Québec. Master's thesis, Université du Québec, Institut national de la recherche scientifique, Québec, Canada
- Beaudry C, Lefebvre R, Rivard C, Cloutier V (2018) Conceptual model of regional groundwater flow based on hydrogeochemistry (Montérégie Est, Québec, Canada). *Can Water Resour J* 43:152–172
- Benoit N, Nastev M, Blanchette D, Molson J (2014) Hydrogeology and hydrogeochemistry of the Chaudière River watershed aquifers, Québec, Canada. *Can Water Resour J* 39:32–48
- Blanchette D, Lefebvre R, Nastev M, Cloutier V (2010) Groundwater quality, geochemical processes and groundwater evolution in the Chateauguay River watershed, Quebec, Canada. *Can Water Resour J* 35:503–526
- Bolduc AM, Ross M (2001) Géologie des formations superficielles, Lachute-Oka, Québec. Geological Survey of Canada, Open File 3520; Natural Resources Canada
- Bondu R, Cloutier V, Rosa E (2018) Occurrence of geogenic contaminants in private wells from a crystalline bedrock aquifer in western Quebec, Canada: Geochemical sources and health risks. *J Hydrol* 559:627–637
- Bondu R, Cloutier V, Rosa E, Roy M (2020) An exploratory data analysis approach for assessing the sources and distribution of naturally occurring contaminants (F, Ba, Mn, As) in groundwater from southern Quebec (Canada). *Appl Geochemistry* 114:1–17
- Boumaiza L, Chesnaux R, Drias T et al (2020) Identifying groundwater degradation sources in a Mediterranean coastal area experiencing significant multi-origin stresses. *Sci Total Environ* 746:1–20
- Boumaiza L, Chesnaux R, Walter J, Meghnefi F (2021) Assessing response times of an alluvial aquifer experiencing seasonally variable meteorological inputs. *Groundw Sustain Dev* 14:1–12. <https://doi.org/10.1016/j.gsd.2021.100647>
- Boumaiza L, Chesnaux R, Walter J, Stumpp C (2020) Constraining a flow model with field measurements to assess water transit time through a vadose zone. *Groundwater*. <https://doi.org/10.1111/gwat.13056>
- Boumaiza L, Chesnaux R, Walter J, Stumpp C (2020) Assessing groundwater recharge and transpiration in a humid northern region dominated by snowmelt using vadose-zone depth profiles. *Hydrogeol J* 28:2315–2329
- Boumaiza L, Chesnaux R, Walter J, Stumpp C (2021b) Numerical assessment of water transit-time through a thick heterogeneous aquifer vadose-zone. In: Proceedings of the 74th Canadian Geotechnical Conference and the 14th Joint CGS/IAH-CNC Groundwater Conference (GeoNiagara-2021b), Niagara Falls, Ontario, Canada. p 6
- Boumaiza L, Rouleau A, Cousineau PA (2015) Estimation de la conductivité hydraulique et de la porosité des lithofaciés identifiés dans les dépôts granulaires du paléodelta de la rivière Valin dans la région du Saguenay au Québec. In: Proceedings of the 68th Canadian Geotechnical Conference, Quebec City, Quebec, Canada. p 9
- Boumaiza L, Rouleau A, Cousineau PA (2017) Determining hydrofacies in granular deposits of the Valin River paleodelta in the Saguenay region of Quebec. In: Proceedings of the 70th Canadian Geotechnical Conference and the 12th Joint CGS/IAH-CNC Groundwater Conference, Ottawa, Ontario, Canada. 8
- Boumaiza L, Rouleau A, Cousineau PA (2019) Combining shallow hydrogeological characterization with borehole data for determining hydrofacies in the Valin River paleodelta. In: Proceedings of the 72nd Canadian Geotechnical Conference, St-John's, Newfoundland, Canada. 8
- Boumaiza L, Walter J, Chesnaux R et al (2021) An operational methodology for determining relevant DRASTIC factors and their relative weights in the assessment of aquifer vulnerability to contamination. *Environ Earth Sci* 80:1–19. <https://doi.org/10.1007/s12665-021-09575-w>
- Boumaiza L, Walter J, Chesnaux R et al (2022) Groundwater recharge over the past 100 years: regional spatiotemporal assessment and climate change impact over the Saguenay-Lac-Saint-Jean region Canada. *Hydrol Process* 36:1–17. <https://doi.org/10.1002/hyp.14526>
- CEAEQ (Centre d'expertise en analyse environnementale du Québec) (2021) Méthodes d'analyses
- CERM-PACES (2013) Résultats du programme d'acquisition de connaissances sur les eaux souterraines de la région Saguenay-Lac-Saint-Jean. Université du Québec à Chicoutimi, Centre d'études sur les ressources minérales
- Chaillou G, Touchette M, Buffin-Bélanger T et al (2018) Hydrogeochemical evolution and groundwater mineralization of shallow aquifers in the Bas-Saint-Laurent region, Québec, Canada. *Can Water Resour J* 43:136–151
- Charette MA, Sholkovitz ER (2006) Trace element cycling in a subterranean estuary: part 2. Geochemistry of the pore water. *Geochim Cosmochim Acta* 70:811–826
- Chesnaux R (2013) Regional recharge assessment in the crystalline bedrock aquifer of the Kenogami Uplands, Canada. *Hydrol Sci J* 58:421–436
- Chesnaux R, Lambert M, Walter J et al (2011) Building a geodatabase for mapping hydrogeological features and 3D modeling of groundwater systems: application to the Saguenay-Lac-St-Jean region. *Canada Comput Geosci* 37:1870–1882
- Chesnaux R, Stumpp C (2018) Advantages and challenges of using soil water isotopes to assess groundwater recharge dominated by snowmelt at a field study located in Canada. *Hydrol Sci J* 63:679–695
- Cloutier V, Lefebvre R, Savard MM et al (2006) Hydrogeochemistry and groundwater origin of the Basses-Laurentides sedimentary rock aquifer system, St. Lawrence Lowlands, Québec. *Canada Hydrogeol J* 14:573–590
- Cloutier V, Lefebvre R, Savard MM, Therrien R (2010) Desalination of a sedimentary rock aquifer system invaded by Pleistocene Champlain Sea water and processes controlling groundwater geochemistry. *Environ Earth Sci* 59:977–994
- Cloutier V, Lefebvre R, Therrien R, Savard MM (2008) Multivariate statistical analysis of geochemical data as indicative of the hydrogeochemical evolution of groundwater in a sedimentary rock aquifer system. *J Hydrol* 353:294–313
- Cui Y, Wei M (2000) Ambient groundwater quality monitoring and assessment in BC: current status and future directions. Groundwater Section, Ministry of Environment, Lands and Parks, British Columbia, Canada
- Deng YM, Wang YX, Ma T (2009) Isotope and minor element geochemistry of high arsenic groundwater from Hangjinhouqi, the Hetao Plain, Inner Mongolia. *Appl Geochemistry* 24:587–599
- Dessureault R (1975) Hydrogéologie du Lac Saint-Jean, partie nord-est. Ministère des richesses naturelles du Québec, Direction générale des eaux, Service des eaux souterraines
- Ding Y, Gao Y, Sun H et al (2011) The relationships between low levels of urine fluoride on children's intelligence, dental fluorosis in endemic fluorosis areas in Hulunbuir, Inner Mongolia, China. *J Hazard Mater* 186:1942–1946
- Elumalai V, Nwabisa DP, Rajmohan N (2019) Evaluation of high fluoride contaminated fractured rock aquifer in South Africa geochemical and chemometric approaches. *Chemosphere* 235:1–11
- Evans AEV, Hanjra MA, Jiang Y et al (2012) Water quality: assessment of the current situation in Asia. *Water Resour Dev* 28:195–216
- Ferroud A, Chesnaux R, Rafini S (2019) Drawdown log-derived analysis for interpreting constant-rate pumping tests in inclined substratum aquifers. *Hydrogeol J* 27:2279–2297

- Ferroud A, Chesnaux R, Rafini S (2018) Insights on pumping well interpretation from flow dimension analysis: the learnings of a multi-context field database. *J Hydrol* 556:449–474
- Foster SSD, Tuinhof A, Garduno H (2006) Groundwater development in Sub-Saharan Africa: a strategic overview of key issues and major needs. The World Bank GW-Mate Case Profile Collection no. 15, World Bank, Washington, DC
- Franklyn MT, McNutt RH, Kamineni DC, Gascoyne M, Frape SK (1991) Groundwater $87\text{Sr}/86\text{Sr}$ values in the Eye-Dashwa Lakes pluton, Canada: Evidence for plagioclase-water reaction. *Chem Geol* 86:111–122
- Ghesquière O, Walter J, Chesnaux R, Rouleau A (2015) Scenarios of groundwater chemical evolution in a region of the Canadian Shield based on multivariate statistical analysis. *J Hydrol Reg Stud* 4:246–266
- Government of Canada (2021) Canada's national climate archive. http://www.climate.weatheroffice.ec.gc.ca/climate_normals/ [consulted in July 2019]
- Grassi S, Netti R (2000) Sea water intrusion and mercury pollution of some coastal aquifers in the province of Grosseto (Southern Tuscany - Italy). *J Hydrol* 237:198–211
- Haines TS, Lloyd JW (1985) Controls on silica in groundwater environments in the United Kingdom. *J Hydrol* 81:277–295
- Hamilton SM, Grasby SE, McIntosh JC, Osborn SG (2015) The effect of long-term regional pumping on hydrochemistry and dissolved gas content in an undeveloped shale-gas-bearing aquifer in southwestern Ontario, Canada. *Hydrogeol J* 23:719–739
- Hanor JS (1994) Origin of saline fluids in sedimentary basins. *Geol Soc London, Spec Publ* 78:151–174
- Health Canada (2020) Guidelines for Canadian Drinking Water Quality-Summary Table. Water and Air Quality Bureau, Healthy Environments and Consumer Safety Branch, Health Canada, Ottawa, Ontario, Canada
- Hounslow AW (1995) Water quality data: analysis and interpretation. Lewis, Boca Raton, FL
- Howard KWF, Haynes J (1993) Groundwater contamination due to road de-icing chemicals — salt balance implications. *Geosci Canada* 20:1–8
- Kendall MG (1975) Rank Correlation Method. Charles Griffin, London
- Kennedy GW, Drage JM (2009) Hydrogeologic characterization of Nova Scotia's groundwater regions. In: The 62nd Canadian Geotechnical Conference and the 10th Joint CGS/IAH-CNC Groundwater Conference. IAH-CNC, Halifax, NS, Canada. 1230–1240
- Khan MMA, Umar R (2010) Significance of silica analysis in groundwater in parts of Central Ganga Plain, Uttar Pradesh, India. *Curr Sci* 98:1237–1240
- Khan A, Umar R, Khan HH (2015) Significance of silica in identifying the processes affecting groundwater chemistry in parts of Kali watershed, Central Ganga Plain, India. *Appl Water Sci* 5:65–72
- Kinsman DJ (1969) Interpretation of Sr^{2+} concentrations in carbonate minerals and rocks. *J Sediment Petrol* 39:486–508
- Koreimann C, Grath J, Winkler G, et al (1996) Groundwater monitoring in Europe. European Environment Agency Copenhagen, Denmark
- Labrecque G, Chesnaux R, Boucher MA (2020) Water-table fluctuation method for assessing aquifer recharge: application to Canadian aquifers and comparison with other methods. *Hydrogeol J* 28:521–533
- Ladevèze P, Rivard C, Lavoie D et al (2019) Fault and natural fracture control on upward fluid migration: insights from a shale gas play in the St. Lawrence Platform. *Canada Hydrogeol J* 27:121–143
- Lamothe M (1989) A new framework for the Pleistocene stratigraphy of the central St. Lawrence Lowland. *Southern Quebec Géographie Phys Quat* 43:119–129
- Lamothe M, St-Jacques G (2014) Géologie du Quaternaire des bassins versant des rivières Nicolet et Saint-François, Québec. Ministère Énergies et Ressources Naturelles, Québec, Canada
- Larocque M, Cloutier V, Levison J, Rosa E (2018) Results from the Quebec groundwater knowledge acquisition program. *Can Water Resour J* 43:69–74
- Lazur A, Van Derwerker T, Koepenick K (2020) Review of implications of road salt use on groundwater quality-corrosivity and mobilization of heavy metals and radionuclides. *Water Air Soil Pollut* 231:1–10
- Leahy PP, Thompson TH (1994) Overview of the National Water-Quality Assessment Program. U.S. Geological Survey Open-File Report 94–70
- Lefebvre R, Ballard JM, Carrier MA, et al (2015) Portrait des ressources en eau souterraine en Chaudière-Appalaches, Québec, Canada. Projet réalisé conjointement par l'Institut national de la recherche scientifique (INRS), l'Institut de recherche et développement en agroenvironnement (IRDA) et le Regrou. Rapport final INRS R-1508, Ministère du Développement durable, de l'Environnement et de la Lutte contre les changements climatiques, Québec, Canada
- Luczaj J, Masarik K (2015) Groundwater quantity and quality issues in a water-rich region: examples from Wisconsin, USA. *Resources* 4:232–357
- Mahlknecht J, Merchán D, Rosner M et al (2017) Assessing seawater intrusion in an arid coastal aquifer under high anthropogenic influence using major constituents, Sr and B isotopes in groundwater. *Sci Total Environ* 587–588:282–295
- Mann HB (1945) Nonparametric tests against trend. *Econometrica* 13:245–259
- McCormack R, Therrien R (2013) St. Lawrence lowlands region. In: Alfonso, R. (Ed.), *Canada's Groundwater Resources*. Fitzhenry & Whiteside. 501–539
- Meinken W, Stober I (1997) Permeability distribution in the Quaternary of the Upper Rhine glacio-fluvial aquifer. *Terra* 9:113–116
- MELCC (Ministère de l'Environnement et de la Lutte contre les changements climatiques) (2021) Projets d'acquisition de connaissance des eaux souterraines. <https://www.environnement.gouv.qc.ca/eau/souterraines/programmes/acquisition-connaissance.htm>
- Meriano M (2007) Groundwater-surface water interaction in Frenchman's bay watershed, Ontario: Implications for urban recharge, contaminant storage and migration. Ph.D. Thesis, University of Toronto, Canada
- Meyzonnat G, Larocque M, Barbecot F et al (2016) The potential of major ion chemistry to assess groundwater vulnerability of a regional aquifer in southern Quebec (Canada). *Environ Earth Sci* 75:1–12
- Middelburg JJ, Van Der Weijden CH, Woittiez JRW (1988) Chemical processes affecting the mobility of major, minor and trace elements during weathering of granitic rocks. *Chem Geol* 68:253–273
- Minet EP, Goodhue R, Meier-Augenstein W et al (2017) Combining stable isotopes with contamination indicators: a method for improved investigation of nitrate sources and dynamics in aquifers with mixed nitrogen inputs. *Water Res* 124:85–96
- Miretzky P, Alicia Fernández C (2004) Silica dynamics in a pampean lake (Lake Chascomús, Argentina). *Chem Geol* 203:109–122
- Moldovanyi E, Walter M, Brannon JC, Podosek FA (1990) New constraints on carbonate diagenesis from integrated Sr and S isotopic and rare earth element data, Jurassic Smackover Formation, U.S. Gulf Coast. *Appl Geochemistry* 5:449–470
- Montcoudiol N, Molson J, Lemieux JM (2015) Groundwater geochemistry of the Outaouais Region (Québec, Canada): a regional-scale study. *Hydrogeol J* 23:377–396

- Moore J, Bird DL, Dobbis SK, Woodward G (2017) Nonpoint Source contributions drive elevated major ion and dissolved inorganic carbon concentrations in urban watersheds. *Environ Sci Technol Lett* 4:198–204
- Mora A, Mahlknecht J, Ledesma-Ruiz R et al (2020) Dynamics of major and trace elements during seawater intrusion in a coastal sedimentary aquifer impacted by anthropogenic activities. *J Contam Hydrol* 323:1–17
- Musgrove ML (2021) The occurrence and distribution of strontium in U.S. groundwater. *Appl Geochemistry* 126:1–18
- Nadeau S, Rosa E, Cloutier V (2018) Stratigraphic sequence map for groundwater assessment and protection of unconsolidated aquifers: A case example in the Abitibi-Témiscamingue region, Québec, Canada. *Can Water Resour J* 43:113–135
- NBDE (New Brunswick Department of Environment) (2008) New Brunswick Groundwater Chemistry Atlas: 1994–2007. Sciences and Reporting Branch, Sciences and Planning Division, Environmental Reporting Series T2008–01
- Oberhelman A, Peterson EW (2020) Chloride source delineation in an urban-agricultural watershed: Deicing agents versus agricultural contributions. *Hydrol Process* 34:4017–4029
- Paalman MAA, Van der Weijden CH, Loch JPG (1994) Sorption of cadmium on suspended matter under estuarine conditions: competition and complexation with major seawater ions. *Water Air Soil Pollut* 73:49–60
- Pohlert T (2020) Non-Parametric Trend Tests and Change-Point Detection. <https://creativecommons.org/licenses/by-nd/4.0/>
- Rango T, Vengosh A, Dwyer G, Bianchini G (2013) Mobilization of arsenic and other naturally occurring contaminants in groundwater of the Main Ethiopian Rift aquifers. *Water Res* 47:5801–5818
- Rey N, Rosa E, Cloutier V, Lefebvre R (2018) Using water stable isotopes for tracing surface and groundwater flow systems in the Barlow-Ojibway Clay Belt, Quebec, Canada. *Can Water Resour J* 43:173–194
- Richard SK, Chesnaux R, Rouleau A, Coupe RH (2016) Estimating the reliability of aquifer transmissivity values obtained from specific capacity tests: examples from the Saguenay-Lac-Saint-Jean aquifers, Canada. *Hydrol Sci J* 61:173–185
- Ricolfi L, Barbieri M, Muteto PV et al (2020) Potential toxic elements in groundwater and their health risk assessment in drinking water of Limpopo National Park, Gaza Province, Southern Mozambique. *Environ Geochem Health* 42:2733–2745
- Rouleau A, Clark ID, Bottomley DJ, Roy DW (2013) Precambrian Shield. In: Alfonso, R. (Ed.), *Canada's Groundwater Resources*. Fitzhenry & Whiteside. 415–441
- Rouleau A, Larocque M, Walter J et al (2012) Le programme d'acquisition de connaissances sur les eaux souterraines, Ses retombées dans les régions de Bécancour et du Saguenay-Lac-Saint-Jean. *Vecteur Environ* 45:30–31
- Russak A, Sivan O, Yechieli Y (2016) Trace elements (Li, B, Mn and Ba) as sensitive indicators for salinization and freshening events in coastal aquifers. *Chem Geol* 441:35–46
- Saby M, Larocque M, Pinti DL et al (2016) Linking groundwater quality to residence times and regional geology in the St. Lawrence Lowlands, southern Quebec. *Canada Appl Geochem* 65:1–13
- Santucci L, Carol E, Kruse E (2016) Identification of palaeo-seawater intrusion in groundwater using minor ions in a semi-confined aquifer of the Rio de la Plata littoral (Argentina). *Sci Total Environ* 566–567:1640–1648
- Seddique AA, Masuda H, Anma R et al (2019) Hydrogeochemical and isotopic signatures for the identification of seawater intrusion in the paleobeach aquifer of Cox's Bazar city and its surrounding area, south-east Bangladesh. *Groundw Sustain Dev* 9:1–12
- Sun H, Alexander J, Gove B, Koch M (2015) Mobilization of arsenic, lead, and mercury under conditions of sea water intrusion and road deicing salt application. *J Contam Hydrol* 180:12–24
- Swartz CH, Blute NK, Badruzzaman B et al (2004) Mobility of arsenic in a Bangladesh aquifer: inferences from geochemical profiles, leaching data, and mineralogical characterization. *Geochim Cosmochim Acta* 68:4539–4557
- Thibaudeau P, Veillette J (2005) Géologie des formations en surface et histoire glaciaire. Commission géologique du Canada, Lac Chicobi, Québec
- Tremblay R, Walter J, Chesnaux R, Boumaiza L (2021) Investigating the potential role of geological context on groundwater quality: a case study of the Grenville and St. Lawrence Platform geological provinces in Quebec. *Canada Geosci* 11:1–21
- Vikas C, Kushwaha R, Ahmad W et al (2013) Genesis and geochemistry of high fluorine-bearing groundwater from a semi-arid terrain of NW India. *Environ Earth Sci* 68:289–305
- Walter J (2018) Modèle d'évolution naturelle de l'eau souterraine dans une région du Bouclier Canadien à partir de la détermination de pôles hydrogéochimiques régionaux. Ph.D Thesis, Université du Québec à Chicoutimi, Québec, Canada
- Walter J, Chesnaux R, Cloutier V, Gaboury D (2017) The influence of water/rock–water/clay interactions and mixing in the salinization processes of groundwater. *J Hydrol Reg Stud* 13:168–188
- Walter J, Chesnaux R, Gaboury D, Cloutier V (2019) Subsampling of regional-scale database for improving multivariate analysis interpretation of groundwater chemical evolution and ion sources. *Geosci* 9:1–32
- Walter J, Rouleau A, Chesnaux R et al (2018) Characterization of general and singular features of major aquifer systems in the Saguenay-Lac-Saint-Jean region. *Can Water Resour J* 43:75–91
- Wen T, Castro MC, Hall CM et al (2015) Constraining groundwater flow in the glacial drift and saginaw aquifers in the Michigan Basin through helium concentrations and isotopic ratios. *Geo-fluids* 16:3–25
- WHO (World Health Organization) (2017) Guidelines for drinking-water quality, 4th edition, incorporating the 1st addendum. ISBN: 978–92–4–154995–0
- Wigley T (1973) The incongruent solution of dolomite. *Geochim Cosmochim Acta* 37:1397–1402
- Williams DD, Williams NE, Cao Y (2000) Road salt contamination of groundwater in a major metropolitan area and development of a biological index to monitor its impact. *Water Res* 34:127–138
- Yadav KK, Kumar V, Gupta N et al (2019) Human health risk assessment: study of a population exposed to fluoride through groundwater of Agra city, India. *Regul Toxicol Pharmacol* 106:68–80
- Yang JY, Wang M, Lu J et al (2020) Fluorine in the environment in an endemic fluorosis area in Southwest, China. *Environ Res* 184:1–10
- Zango MS, Sunkari ED, Abu M, Lermi A (2019) Hydrogeochemical controls and human health risk assessment of groundwater fluoride and boron in the semiarid North East region of Ghana. *J Geochemical Explor* 207:1–21
- Zendehbad M, Cepuder P, Loiskandl W, Stumpp C (2019) Source identification of nitrate contamination in the urban aquifer of Mashhad. *Iran J Hydrol Reg Stud* 25:1–14

Publisher's note Springer Nature remains neutral with regard to jurisdictional claims in published maps and institutional affiliations.